International Journal of Nanomedicine

Dovepress
open access to scientific and medical research

Open Access Full Text Article

ORIGINAL RESEARCH

Inducing cell cycle arrest and apoptosis by dimercaptosuccinic acid modified Fe_3O_4 magnetic nanoparticles combined with nontoxic concentration of bortezomib and gambogic acid in RPMI-8226 cells

This article was published in the following Dove Press journal:
International Journal of Nanomedicine
30 April 2015
Number of times this article has been viewed

Wei Zhang[1,*]
Lixing Qiao[2,*]
Xinchao Wang[3,*]
Ravichandran Senthilkumar[1]
Fei Wang[1]
Baoan Chen[1,4]

[1]Medical School, Southeast University, Nanjing, People's Republic of China; [2]Department of Pediatrics, Zhongda Hospital, Medical School, Southeast University, Nanjing, People's Republic of China; [3]Department of Thyroid and Breast, the Fourth Central Hospital, Tianjin, People's Republic of China; [4]Department of Hematology and Oncology, Zhongda Hospital, Medical School, Southeast University, Nanjing, People's Republic of China

*These authors contributed equally to this work

Abstract: The purpose of this study was to determine the potential benefits of combination therapy using dimercaptosuccinic acid modified iron oxide (DMSA-Fe_3O_4) magnetic nanoparticles (MNPs) combined with nontoxic concentration of bortezomib (BTZ) and gambogic acid (GA) on multiple myeloma (MM) RPMI-8226 cells and possible underlying mechanisms. The effects of BTZ-GA-loaded MNP-Fe_3O_4 (BTZ-GA/MNPs) on cell proliferation were assessed by the 3-(4,5-dimethylthiazol-2-yl)-2,4,-diphenyltetrazolium bromide (MTT) method. Cell cycle and apoptosis were detected using the terminal deoxyribonucleotidyl transferase (TdT)-mediated biotin-16-dUTP nick-end labeling (TUNEL) assay and flow cytometry (FCM). Furthermore, DMSA-Fe_3O_4 MNPs were characterized in terms of distribution, apoptotic morphology, and cellular uptake by transmission electron microscopy (TEM) and 4,6-diamidino-2-phenylindole (DAPI) staining. Subsequently, the effect of BTZ-GA/MNPs combination on PI3K/Akt activation and apoptotic-related protein were appraised by Western blotting. MTT assay and hematoxylin and eosin (HE) staining were applied to elevate the functions of BTZ-GA/MNPs combination on the tumor xenograft model and tumor necrosis. The results of this study revealed that the majority of MNPs were quasi-spherical and the MNPs taken up by cells were located in the endosome vesicles of cytoplasm. Nontoxic concentration of BTZ-GA/MNPs increased G_2/M phase cell cycle arrest and induced apoptosis in RPMI-8226 cells. Furthermore, the combination of BTZ-GA/MNPs activated phosphorylated Akt levels, Caspase-3, and Bax expression, and down-regulated the PI3K and Bcl-2 levels significantly. Meanwhile, the in vivo tumor xenograft model indicated that the treatment of BTZ-GA/MNPs decreased the tumor growth and volume and induced cell apoptosis and necrosis. These findings suggest that chemotherapeutic agents polymerized MNPs-Fe_3O_4 with GA could serve as a better alternative for targeted therapeutic approaches to treat multiple myeloma.

Keywords: magnetic nanoparticles, DMSA-Fe_3O_4, bortezomib, gambogic acid, PI3K/Akt, cell cycle, apoptosis

Introduction

Multiple myeloma (MM) is a malignant disease of the terminally differentiated B-cell.[1–3] Although the therapeutic arsenal has been enlarged by the introduction of novel agents such as bortezomib (BTZ) and lenalidomide, MM still remains an incurable hematologic disorder.[3,4] BTZ is a specific 26S reversible proteasome inhibitor that remains the first-line treatment for MM patients. It has been demonstrated that the synergetic drug combinations of BTZ with adriamycin and dexamethasone[5,6]

Correspondence: Baoan Chen
Department of Hematology and Oncology, Zhongda Hospital, Medical School, Southeast University, 87 DingjiaQiao Road, Nanjing 210009, People's Republic of China
Tel +86 25 8327 2006
Fax +86 25 8327 2011
Email cba8888@hotmail.com

yields remarkable anti-MM activities in both preclinical[7,8] and clinical studies.[9,10] However, MM patients treated with a higher dose of BTZ with doxorubicin or dexamethasone are affected by adverse side effects, which are a serious problem in oncotherapy.[11,12] Therefore, in order to reduce the chemoresistance and complications while maintaining good antitumor activity, a lower dose of BTZ in combination with a second or third agent would be a common strategy.

Gambogic acid (GA), a main active ingredient of gamboge, is a brownish to orange dry resin secreted from *Garcinia hanburyi*, a plant that is widely distributed in nature. Recently, several studies have demonstrated that GA has potent antitumor effects on solid tumors and hematological malignancies.[13] GA has been approved by the Chinese Food and Drug Administration for clinical trials in cancer patients.[14] In addition, it is reported that GA mediates a wide variety of functional antitumor effects, including the induction of cell apoptosis, inhibition of proliferation, and prevention of cancer metastasis and angiogenesis. Hence, previous investigations suggest that GA might be an effective anticancer drug candidate with low toxicity to normal cells.[15,16] However, several drawbacks such as the poor aqueous solubility and wide tissue distribution limited its usefulness in cancer therapy, and have a great impact on the development of pharmaceutical preparations and clinical application.

Nanoparticle-based drug delivery systems have shown a potential to enhance the accumulation of anticancer agents in tumor cells.[17,18] MNPs-Fe_3O_4 has been one of the major drug delivery systems over recent years. The application of MNPs-Fe_3O_4 is widespread in various biomedical fields such as enhanced resolution magnetic resonance imaging (MRI), drug delivery, tissue repair, molecular/cellular tracking, cell separation, tissue targeting, and transfection.[19–24] The hydrodynamic size of MNPs-Fe_3O_4 modified with dimercaptosuccinic acid (DMSA), ranging from 10 to 100 nm, can prevent tissue extravasation, renal clearance and avoid being quickly opsonized, eliminated from circulation via the reticuloendothelial system. To the best of our knowledge, no study has been carried out on MNPs-Fe_3O_4 nanoparticles combined with nontoxic concentration of BTZ and GA to treat MM RPMI-8226 cells. Here, we investigated for the first time the feasibility of nontoxic concentration of BTZ with GA-polymerized MNPs (BTZ-GA/MNPs) as a drug delivery system for combination cancer chemotherapy. The DMSA-modified MNPs-Fe_3O_4 were characterized for morphology, distribution, and cellular uptake by transmission electron microscopy (TEM) studies. Furthermore, the possible signaling pathway of apoptotic induction and cell cycle arrest were explored in RPMI-8226 cells in vitro by molecular techniques. Finally, the therapeutic efficiency of BTZ-GA/MNPs in vivo antitumor activity was assessed in the tumor-bearing nude mouse model.

Materials and methods

Materials

DMSA-coated MNPs-Fe_3O_4 were prepared as previously described.[25] Average hydrodynamic size of aggregates of DMSA-Fe_3O_4 dispersed in Roswell Park Memorial Institute (RPMI) 1640 medium (Gibco, USA) containing 10% (v/v) inactivated fetal calf serum (Sijiqing Biological Engineering Materials Co., Ltd., Hangzhou, People's Republic of China) is 68.4 nm.[26] BTZ was obtained from Janssen-Cilag (Neuss, Germany). GA was purchased from Jiangsu Kanion Pharmaceutical Co., Ltd (Lianyungang, Jiangsu Province, People's Republic of China). Other reagents used include 3,-(4,5-dimethyl-2-thiazolyl)-2,5-diphenyl-2-tetrazolium bromide (MTT) (Sigma-Aldrich, St Louis, MO, USA), Annexin V-fluorescein isothiocyanate Apoptosis Detection kit, terminal deoxyribonucleotidyl transferase (TdT)-mediated biotin-16-dUTP nick-end labeling (TUNEL) assay kit (KeyGen Biotech Co., Ltd., Nanjing, People's Republic of China), and 4,6-diamidino-2-phenylindole (DAPI) staining solution and hematoxylin and eosin (HE) staining (Beyotime Institute of Biotechnology, Jiangsu, People's Republic of China), monoclonal antibodies, including PI3K, total-Akt and phospho-Akt, Caspase-3, Bcl-2, and Bax, as well as all secondary antibodies such as goat anti-mouse, goat anti-rabbit, and bovine anti-goat immunoglobulins were all purchased from Santa Cruz Biotechnology (Dallas, TX, USA).

Preparation of BTZ-GA/MNPs

DMSA-Fe_3O_4 was provided by Jiangsu Key Laboratory for Biomaterials and Devices of the biomedical system laboratories of Southeast University.[27] Different weights of DMSA-Fe_3O_4 (5, 10, 20, 40, 60, or 80 mg/L) were well dispersed in RPMI 1640 medium supplemented with 10% heat-inactivated fetal bovine serum (FBS) before applying in the present experiment.[28] The various concentrations of GA (0.2, 0.4, 0.8, 1.6, 3.2, or 6.4 μM) or BTZ (2.5, 5, 10, 20, 40, or 60 nM) was dissolved in DMSO, respectively. Various solutions containing one or both drugs were added into the aqueous dispersion of DMSA-Fe_3O_4 to get the mixture. Then, it was kept below 4°C for 48 hours to enable the drugs to conjugate with the MNPs by mechanical absorption polymerization.[29,30]

Cell line and cell culture

Human MM RPMI-8226 cell line was obtained from Jiangsu Institute of Hematology (Suzhou, People's Republic of China). The cells were cultured in RPMI 1640 medium

with 10% FBS, 100 U/mL penicillin, and 100 μg/mL streptomycin at 37°C in a 5% carbon dioxide humidified environment. Cells in logarithmic growth phase were used in all experiments.

MTT assay

Cell cytotoxicity was measured by the MTT assay in vitro. Briefly, RPMI-8226 cells were seeded onto 96-well plates at a density of 4×10^4 cells/mL and grown to 70%–80% confluency, respectively. Twenty-four hours later, cells were treated with medium containing different compounds at indicated concentrations for 48 hours: MNPs (0–80 mg/L), BTZ (0–60 nM), and GA (0–6.4 μM), respectively. The absorbance was read at 570 nm in a microplate reader (Thermo Scientific Multiskan MK3; Boston, MA, USA). The cell inhibition ratio (%) was calculated as: (1-OD treated cells/OD control cells) ×100%. Finally, dose-effect curves were plotted and IC50 values were calculated.

Cell cycle determination

The RPMI-8226 cells were seeded in six-well plates at a density of 2×10^6 cells/well. Cells were treated with control, DMSA-Fe_3O_4 (60 mg/L), BTZ (2.5 nM), GA (0.2 μM), combination of BTZ-GA, and combination of BTZ-GA/MNPs for 48 hours. Thereafter, cells were collected and fixed in ice-cold 70% ethanol and stored at 4°C overnight. Prior to analysis, the cells were washed twice with phosphate-buffered saline (PBS) (0.01 M, pH 7.4), and suspended in 0.5 mL of cold propidium iodide (PI) solution containing 10 μL RNase A (25 μg/mL), 10 μL PI (50 μg/mL). Then cells were incubated at 37°C for an additional 30 minutes in the dark, and determined by analyzing 15,000 ungated cells using a FACScan cytometer and Cell Quest software (FACSCalibur; Becton-Dickinson, San Jose, CA, USA).

Assessment of apoptosis

The RPMI-8226 cells were seeded in six-well plates at a density of 2×10^6 cells/well and treated as described in cell cycle analysis and incubated for 48 hours. Harvested cells were added with 0.01 M CD34-FITC and kept for 15 minutes. Labeled cells were washed thrice with PBS. Thereafter, cells were suspended by 400 μL PBS and determined by a FACS Calibur flow cytometry (FCM) (Becton-Dickinson, Franklin Lakes, NJ, USA) at excitation and emission wavelengths of 488 nm and 575 nm, respectively.

Western blot analysis

Whole-cell lysates from RPMI-8226 cells were prepared. The amount of cellular protein was measured by the method proposed by Lowry et al[31] and stored at −80°C prior to use. Twenty microgram of protein of each sample was separated on SDS-PAGE gels as previously described.[32] After electrophoresis, the proteins were transferred onto polyvinylidene difluoride (PVDF) membranes. After blocking with Tris-buffered saline 0.05% Tween-20 containing 5% skim milk or 3% bovine serum albumin (Sigma, St Louis, MO, USA), blots were incubated at 4°C overnight with the primary rabbit polyclonal or monoclonal antibodies against human PI3K (1:1,000), Akt (1:500), phospho-Akt ($pSer^{473}$, 1:500), Caspase-3 (1:2,000), Bcl-2 (1:500), and Bax (1:500) (Cell Signaling Technology, Danvers, MA, USA), respectively. Membranes were reprobed with anti β-actin antibody (1:1,000; Sigma, St Louis, MO, USA) as loading control. Horseradish peroxidase (HRP)-conjugated sheep anti-rabbit or mouse immunoglobulins were used as a secondary antibody (Sigma, St Louis, MO, USA). The bounded antibody was detected by enhanced chemiluminescence using Immobilon Western reagents (Millipore, Billerica, MA, USA) and exposed to X-ray film according to the manufacturer's protocol.

DAPI staining

The RPMI-8226 cells were treated following the above-mentioned methods for 48 hours, and were then fixed with 4% polyoxymethylene prior to washing with PBS. The washed cells were then stained with 1 mg/mL DAPI for 15 minutes in the dark. Staining images were recorded with a fluorescent microscope.

TEM assay

TEM analysis was used to investigate the intracellular localization of the DMSA-Fe_3O_4 inside the cells. The cells were seeded on a six-well plate at a density of 5.0×10^5 cells/well and cultured for 24 hours. Then the cells were exposed to the DMSA-Fe_3O_4 (60 mg/L) for 24 hours. At the predetermined time, the cells were collected, washed three times with PBS, pelleted using centrifugation, and fixed in 2.5% glutaraldehyde for 2 hours. After pellets were washed by PBS, postfixation with 1% osmium tetroxide was performed. Finally, the pellets were dehydrated with an ascending series of alcohols before embedding the samples in araldite. The specimens were cut into ultrathin sections (50–70 nm), which were placed onto copper grids and stained with uranyl acetate and lead citrate. The ultrastructural analysis was performed using a JEM-1011EX instrument (JEOL, Tokyo, Japan).

Xenograft mouse tumor model

In vivo antitumor activity of the BTZ or GA alone or in combination with MNPs was evaluated in the subcutaneous RPMI-8226 tumor-bearing nude mouse model. Six-week-old

male BALB/c nude mice, with body weights of 18–22 g, were procured from Shanghai National Center for Laboratory Animals (Shanghai, People's Republic of China) and maintained in a specific pathogen-free environment where temperature was maintained at 22°C and humidity in the range of 40%–50%. Studies involving these mice were performed in adherence with the Guidelines established by the National Science Council, People's Republic of China. When the tumor volume reached approximately 100 mm^3 (approximately 10 days), mice were randomly divided into six groups with six mice in each group: normal saline group (0.2 mL, daily), MNPs group (0.75 mg/kg, daily), BTZ group (0.25 mg/kg, weekly once), GA group (2 mg/kg, once every other day), combination of BTZ (0.25 mg/kg, weekly once)–GA group (2 mg/kg, once every other day), and combination of BTZ (0.25 mg/kg, weekly once)–GA group (2 mg/kg, once every other day)/MNPs (0.75 mg/kg, daily). The therapy was continued for 18 days through vena caudalis injection, respectively. Tumor sizes were measured once every other day by using a Vernier caliper and tumor volumes were calculated by using the formula, V =0.5× length × width[2,32] where V is tumor volume (mm^3). The weight of each mouse was measured and ratios of tumor volume to total weight were calculated at each time point. After 18 days, the mice were sacrificed, and the tumor xenografts were removed and measured, and sectioned for TUNEL assays using HE staining.

TUNEL assay

The DeadEnd Colorimetric TUNEL assay kit (Promega, Madison, WI, USA) was used to determine apoptotic cells in tumor sections, according to the manufacturer's protocols. This assay measures biotinylated nucleotide incorporation in DNA, which was then visualized by HRP-labeled streptavidin and DAB. Staining was visualized by Eclipse E-400 microscope and images were captured from four different fields in each tumor section. Three slides were generated from each tumor in each group, and then ten fields from each slide were randomly selected to perform statistical analysis.

Histopathological morphology analysis

All histopathological tests were performed using standard laboratory procedures.[32] The tumor tissues were embedded in paraffin blocks, sliced into 5 mm thick sections, and placed onto glass slides. After HE staining, the slides were observed and photographs were taken using an optical microscope (Motorized inverted system microscope IX81/IX81–ZDC; Olympus, Tokyo, Japan). The pathologist performing the visual analysis was blinded to the sample identifier and results of the other histopathological analyses.

Statistical analysis

All experiments were performed three times. Data were expressed as mean ± standard deviation, and analyzed with SPSS software (version 13.0; SPSS Inc., Chicago, IL, USA). Differences were evaluated using one-way analysis of variance or Student's *t*-test. A value of $P<0.05$ denoted statistical significance.

Results

Inhibition of cell proliferation

The MTT assay was carried out to explore the cell proliferation of human MM RPMI-8226 cells. The cells were subjected to different concentrations of DMSA-Fe_3O_4 (0–80 mg/L), BTZ (0–60 nM), GA (0–6.4 μM), BTZ-GA, or BTZ-GA/MNPs for 48 hours (Figure 1A–D), respectively. The results revealed that MNPs alone had no obvious cytotoxic effect on RPMI-8226 cells until the concentration of MNPs reached 60 mg/L. Nevertheless, the cell growth inhibition rate was 32.84% when the concentration of MNPs exceeded 60 mg/L (Figure 1A). BTZ at 5 nM led to a significant inhibition of cell growth (approximately 28.25%) and increased concentrations of BTZ enhanced the inhibition of cell growth. A similar phenomenon was observed for GA at 0.4 μM, exhibiting an inhibitory effect (30.31%) on RPMI-8226 cell growth in a dose-dependent manner. However, nontoxic concentration of BTZ at 2.5 nM or GA at 0.2 μM did not lead to the inhibition of cell growth. Interestingly, the combination of BTZ (2.5 nM) and GA (0.2 μM) significantly inhibited cell growth (Figure 1D). The low-concentration combinations of BTZ (2.5 nM)–GA (0.2 μM) and high-concentration combinations of BTZ (5 nM)–GA (0.4 μM) with or without MNPs (0–80 mg/L) exhibited a more pronounced growth inhibitory effect on RPMI-8226 cells than any drugs alone did ($P<0.05$, Figure 1D). Furthermore, MNPs at the dose of 60 mg/L combined with nontoxic concentration of BTZ-GA on RPMI-8226 cells had a higher inhibition ratio compared with that of the BTZ-GA group ($P<0.05$, Figure 1D).

Characterization of DMSA-Fe_3O_4 MNPs and BTZ-GA/MNPs

The ultrastructural changes of DMSA-Fe_3O_4 were observed using TEM. As shown in Figure 2A, a majority of MNPs were quasi-spherical with an average diameter of 18.7±5.61 nm, compared with the untreated RPMI-8226 cells

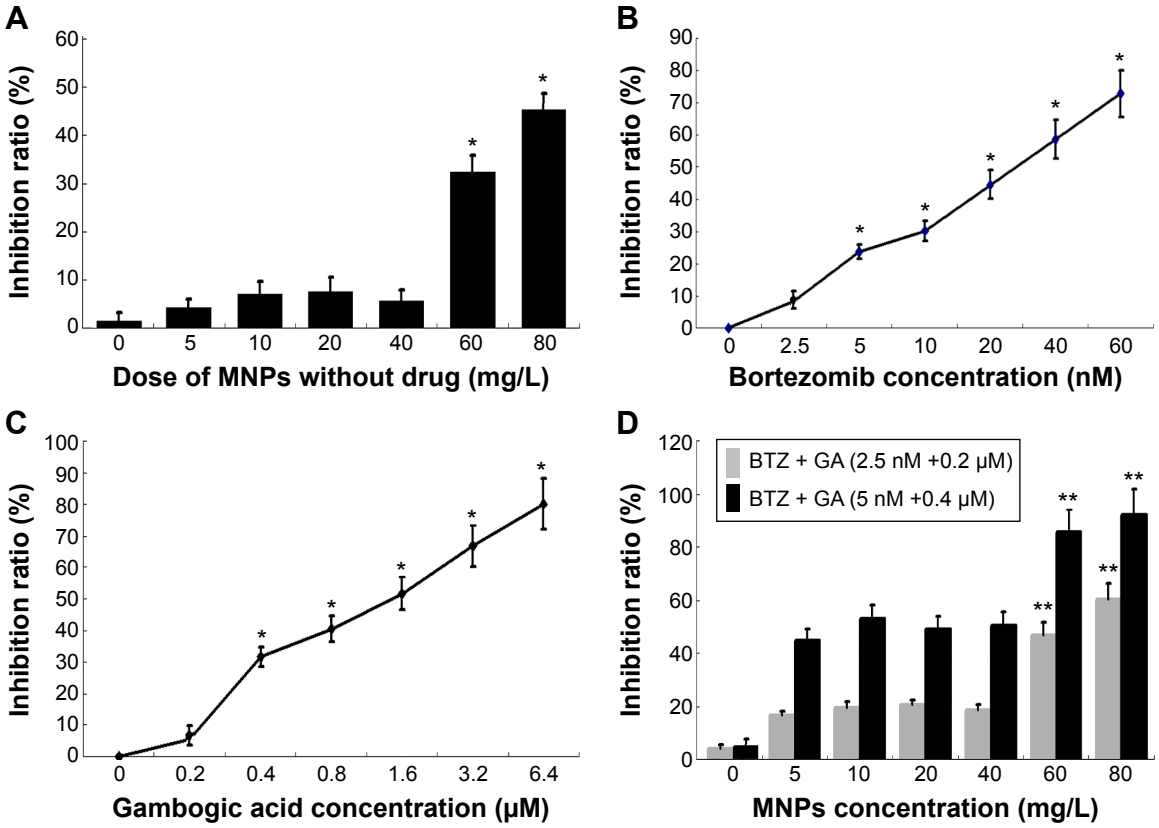

Figure 1 Inhibition ratio of RPMI-8226 cells treated with different concentrations of MNPs (**A**) BTZ, (**B**) GA, (**C**) BTZ-GA, or MNPs combined with BTZ-GA (**D**) for 48 hours.
Notes: *$P<0.05$, compared with the other concentration; **$P<0.05$, when compared with the BTZ-GA group.
Abbreviations: DMSA-Fe_3O_4 MNPs, dimercaptosuccinic acid modified iron oxide magnetic nanoparticles (MNPs); BTZ, bortezomib; GA, gambogic acid; BTZ-GA, bortezomib-gambogic acid; BTZ-GA/MNPs, bortezomib-gambogic acid/dimercaptosuccinic acid modified iron oxide (DMSA-Fe_3O_4) magnetic nanoparticles.

(Figure 2B), MNPs located in the endosome vesicles of the cytoplasm of RPMI-8226 cells (Figure 2C–D). MNPs were synthesized by chemical coprecipitation and a stable MNP suspension was obtained via surface coating with DMSA,[26] which polymerized the lower concentration BTZ and GA. Figure 3 shows a schematic representation of synthesized BTZ-GA/MNPs nanocomposites.

Cell cycle arrest

The effects of DMSA-Fe_3O_4 (60 mg/L), BTZ (2.5 nM), GA (0.2 μM), combination of BTZ-GA, and combination of BTZ-GA/MNPs on the cell cycle were investigated by FCM at 48 hours. Results showed an increased amount of the cell population in the G_2/M phase in the BTZ-GA/MNPs group (44.78%±5.31%), compared with the other groups ($P<0.05$). Interestingly, the number of cells in the combination of BTZ-GA group (33.68%±4.27%) was greater than in groups with BTZ (13.32%±3.41%) or GA (17.45%±2.19%) alone ($P<0.05$). Furthermore, there were slight increases in the concentrations of BTZ at 2.5 nM and GA at 0.5 μM alone as compared to the control group. However, there was no significant difference between MNPs alone (11.71%±2.18%) and the control group (8.95%±0.94%) ($P>0.05$). According to this result, we infer that DMSA-Fe_3O_4 alone could potentially induce cell cycle arrest in the G_2/M phase. Furthermore, a combination of nontoxic concentration of BTZ and GA revealed a better synergistic effect on RPMI-8226 cells (Figure 4A–F).

Enhancement of cell apoptosis

Apoptotic rates of RPMI-8226 cells were examined with Annexin V staining assay by FCM. Cell apoptosis was observed in the BTZ-GA combination group (24.86%±2.19%) and the BTZ-GA/MNPs combination group (70.65%±6.03%). The combination treatment significantly increased the apoptotic rates when compared with the BTZ (10.52%±1.41%) or GA alone (8.01%±0.87%) ($P<0.05$, Figure 5A–F). Consequently, the BTZ-GA/MNPs group showed a higher apoptotic rate than the BTZ-GA group ($P<0.05$, Figure 5E–F). Furthermore, there were typical features of variable extent of apoptosis such as chromatin condensation, nucleolus pyknosis, nuclear fragmentation, and apoptotic bodies

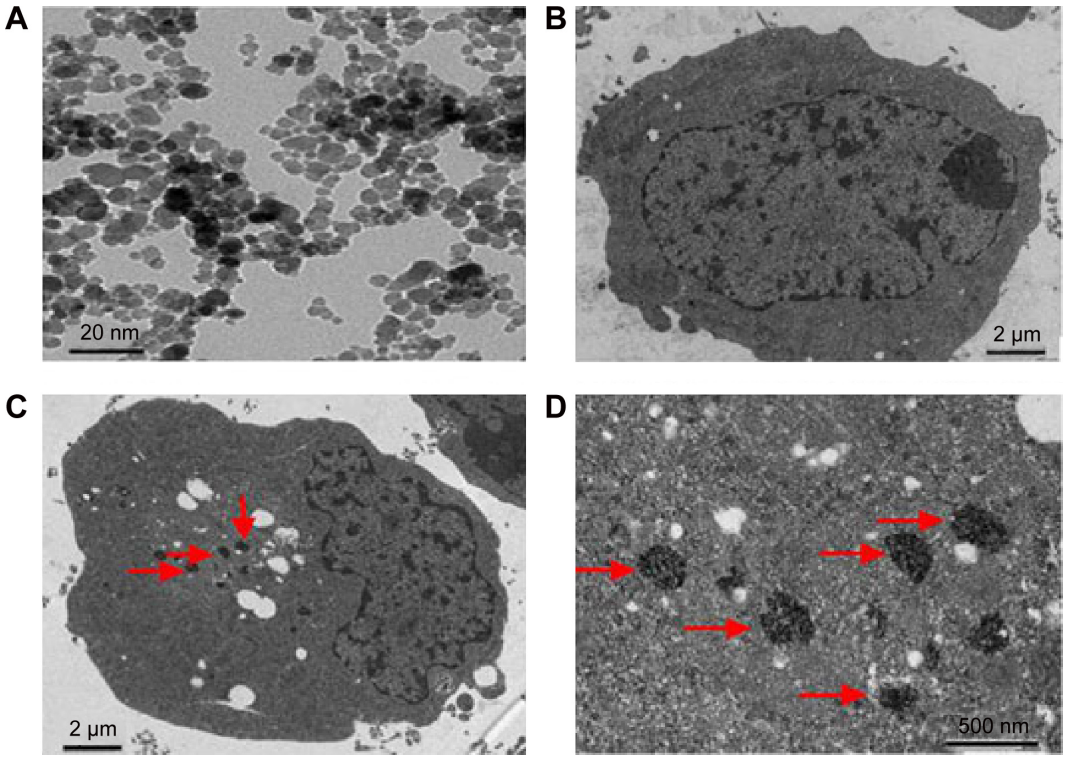

Figure 2 TEM images of MNPs. (**A**) DMSA-Fe_3O_4; distribution of nanoparticles in RPMI-8226 cells treated with or without MNPs for 48 hours by TEM. (**B**) without MNPs (**C**) with MNPs. (**D**) Magnification 5× (**C**).
Note: Red arrows depict MNPs in the endosome vesicles.
Abbreviations: TEM, transmission electron microscopy; DMSA-Fe_3O_4 MNPs, dimercaptosuccinic acid modified iron oxide magnetic nanoparticles.

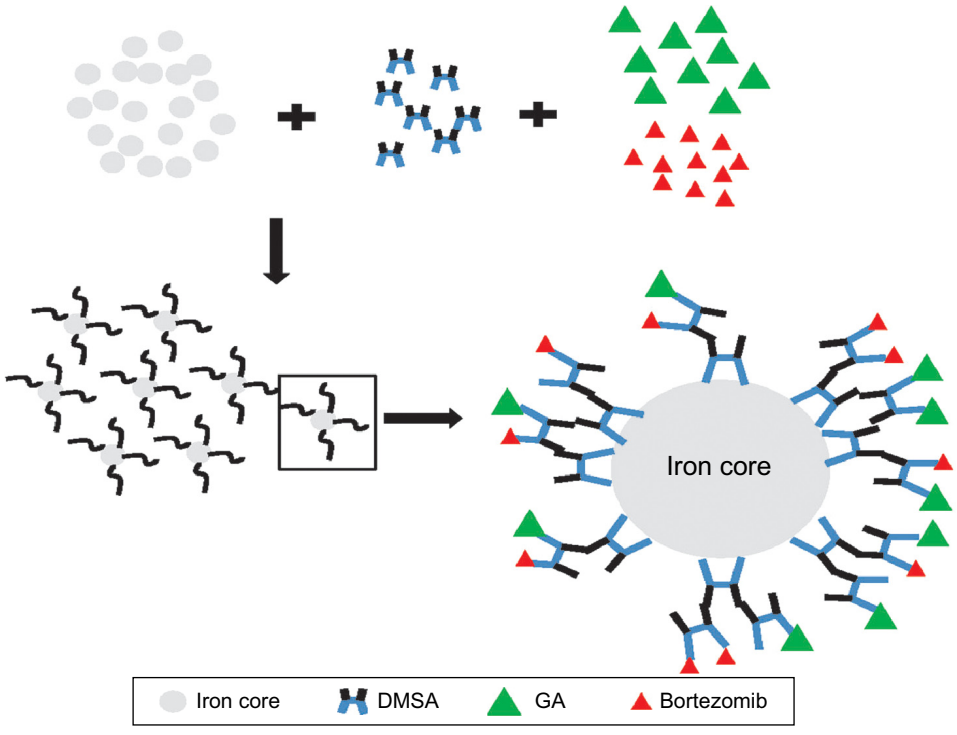

Figure 3 Schematic representation of BTZ with GA polymerized DMSA modified iron oxide magnetic nanoparticles (MNPs) through the formation of bortezomib-gambogic acid DMSA-Fe_3O_4 MNP nanocomposites.
Abbreviations: Iron core, iron oxide core; BTZ, bortezomib; GA, gambogic acid; DMSA, dimercaptosuccinic acid; DMSA-Fe_3O_4, dimercaptosuccinic acid modified iron oxide; MNPs, magnetic nanoparticles.

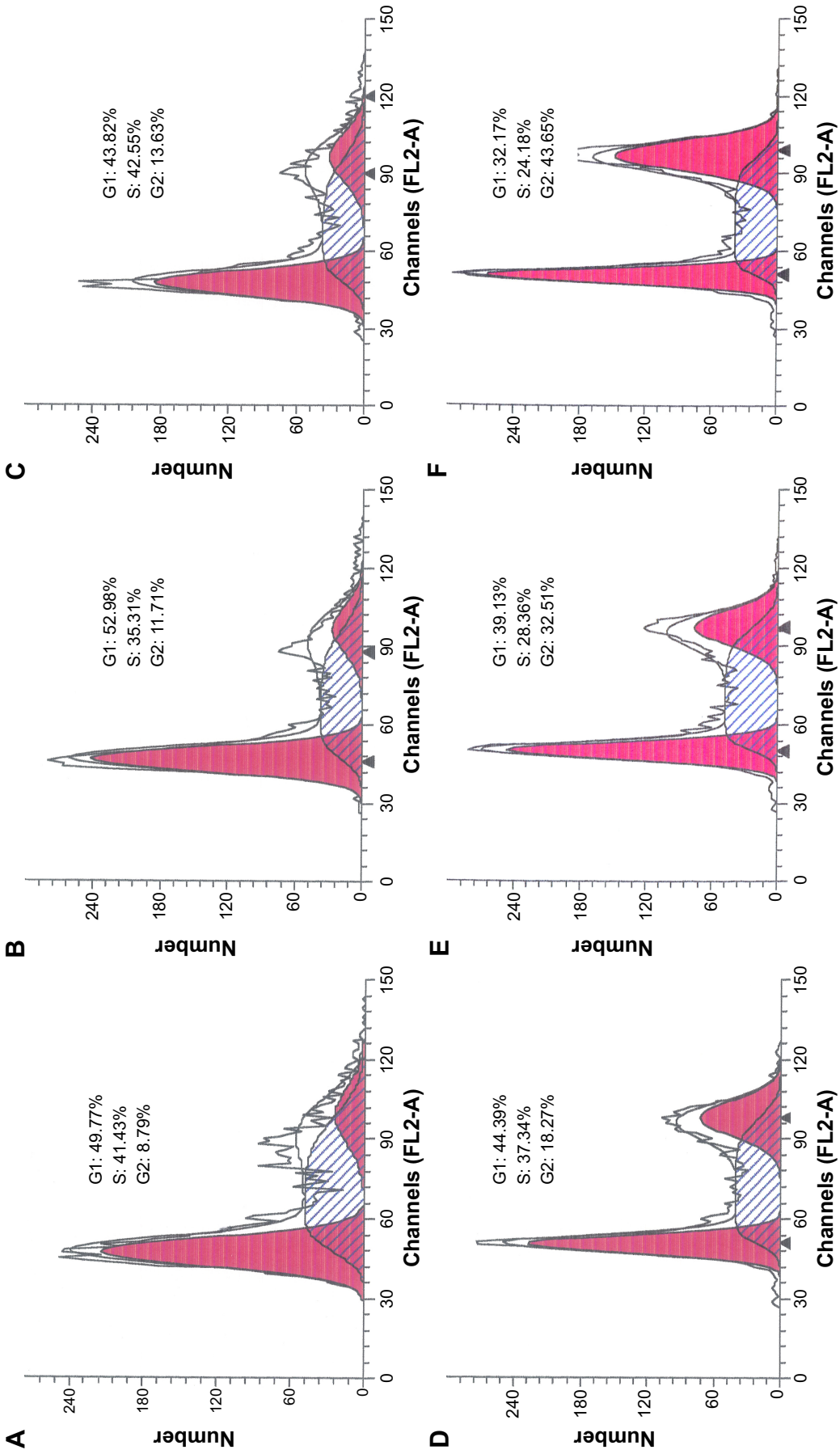

Figure 4 Cell cycle determination of RPMI-8226 cells for 48 hours by FCM assay. (**A**) control; (**B**) 60 mg/L DMSA-Fe_3O_4; (**C**) 2.5 nM BTZ; (**D**) 0.2 μM GA; (**E**) 2.5 nM BTZ-0.2 μM GA; (**F**) 2.5 nM BTZ-0.2 μM GA-60 mg/L DMSA-Fe_3O_4.

Abbreviations: FCM, flow cytometry; DMSA-Fe_3O_4, dimercaptosuccinic acid modified iron oxide; BTZ, bortezomib; GA, gambogic acid; BTZ-GA, bortezomib-gambogic acid; BTZ-GA/MNPs, bortezomib-gambogic acid/dimercaptosuccinic acid modified iron oxide (DMSA-Fe_3O_4) magnetic nanoparticles.

(Figure 6E–F). Interestingly, there was no significant difference between DMSA-Fe_3O_4 alone (6.28%±0.91%), BTZ alone (9.96%±1.04%) and GA alone (8.31%±0.84%) as shown in Figure 6B–D compared with the control group (4.86%±0.68%, Figure 6A), though there is increase trend of cell apoptosis among these groups. All these results further strengthen the possibility that MNPs could reinforce the combined effects of BTZ-GA on cell apoptosis.

Expression of cell apoptotic-related proteins

Protein expression of RPMI-8226 cells treated with either BTZ or GA or a combination of BTZ-GA/MNPs as in the above-mentioned corresponding treatment for 48 hours were subjected to computer-assisted image analysis. As shown in Figure 7, the expression levels of PI3K, Akt, pSer^{473}, and Bcl-2 proteins were down-regulated in BTZ-GA or BTZ-GA/MNPs combination groups. Meanwhile, the expressions of proapoptotic proteins such as Caspase-3 and Bax protein were higher in the BTZ-GA/MNPs group, compared with the other groups ($P<0.05$). Furthermore, a slightly increased expressions of Caspase-3 and Bax proteins were observed in BTZ or GA alone, compared with the control group ($P<0.05$). In addition, the protein expression of RPMI-8226 cells in the DMSA-Fe_3O_4-treated group did not change obviously when compared with the control group ($P>0.05$, Figure 7).

In vivo antitumor activity

The change in the mice body weight status was recorded to evaluate the toxicity of the combination of MNPs with BTZ and GA in RPMI-8226 cells. As shown in Figure 8A–C, the tumor size, body weight, and volume of the mice in the BTZ-GA group and the BTZ-GA/MNPs combination group were significantly decreased than that of the BTZ or GA alone. The results revealed that the BTZ-GA/MNPs-treated group had significant antitumor efficacy as compared to the other groups ($P<0.05$). In addition, there was no significant difference in the weight decrease ratio with BTZ or GA alone ($P>0.05$). These results demonstrate again that the low concentration of BTZ or GA alone did not show antitumor activity in tumor tissues efficiently.

Induction of cell apoptosis and necrosis in xenograft tumors

A mouse model of human MM (RPMI-8226) was used to assess the combinatorial efficacy of drug-loaded MNPs-Fe_3O_4 for inhibition of tumor growth. Stocks of MM tumors were established by subcutaneously injecting RPMI-8226 cells in the flank of nude mice. The synergistic effect of BTZ or GA or the combination of BTZ-GA/MNPs on the apoptosis induction in the xenograft tumors excised from mice was evaluated by TUNEL staining. As depicted in Figure 9A and B, the apoptotic cells in the RPMI-8226 xenograft tumors of control or MNPs groups were approximately 4.23%±0.33% or 2.61%±0.08%. A slight increase in apoptotic cells was observed with BTZ (10.12%±2.67%) or GA (13.02%±3.01%) alone. However, as shown in Figure 9B, there were more apoptotic cells in the xenografts of the BTZ-GA group (28.46%±2.33%) or the BTZ-GA/MNPs combination group (42.36%±3.15%). The number of apoptotic cells in the BTZ-GA/MNPs group was considerably higher compared to that of the control or MNPs groups alone. Similar results of tumor tissues in necrosis were observed in the BTZ-GA group or the BTZ-GA/MNPs group by HE staining. In addition, a major area of tumor necrosis was observed in the BTZ-GA/MNPs combination group as compared with the other groups ($P<0.05$, Figure 10). However, a few tumor necrotic cells were observed in GA alone as compared with the control group.

Discussion

MNPs of Fe_3O_4 (MNPs-Fe_3O_4), a biocompatible and superparamagnetic nanomaterial, is widely used for targeted-drug carriers with lower toxicity and controlled drug release. Chen et al has introduced MNPs-Fe_3O_4 to deliver GA to K562 human leukemia cell lines, and it was found that GA inhibited the proliferation of leukemia cells remarkably by a higher expression levels of *Caspase-3* and *Bax* genes.[33] In the present study, we explored the combinatorial chemotherapeutic efficacy of DMSA-Fe_3O_4 (60 mg/L) and BTZ (2.5 nM) with GA (0.2 μM) (BTZ-GA/MNPs) in MM in vitro model, RPMI-8226 cell line. This combined regimen significantly suppressed PI3K/Akt activation and increased G_2/M phase cell cycle arrest to bring down cellular apoptosis. Furthermore, tumor growth was delayed and enhanced necrosis occurred in vivo. The combination of BTZ-GA/MNPs showed potent effects on growth inhibition, cell cycle arrest, and apoptosis in RPMI-8226 cells. In addition, experiments on the animal model proved that this combination regimen has minimal toxicity and efficient antitumor activity.

The accumulated data has demonstrated that GA possesses broad spectrum of antitumor activity against in vitro and in vivo cancer models by down-regulating telomerase activity, and inducing apoptotic cascade.[34,35] Furthermore, our previous data reported that GA has no toxicity at the concentrations of both 0.025 μM and 0.4 μM in U266

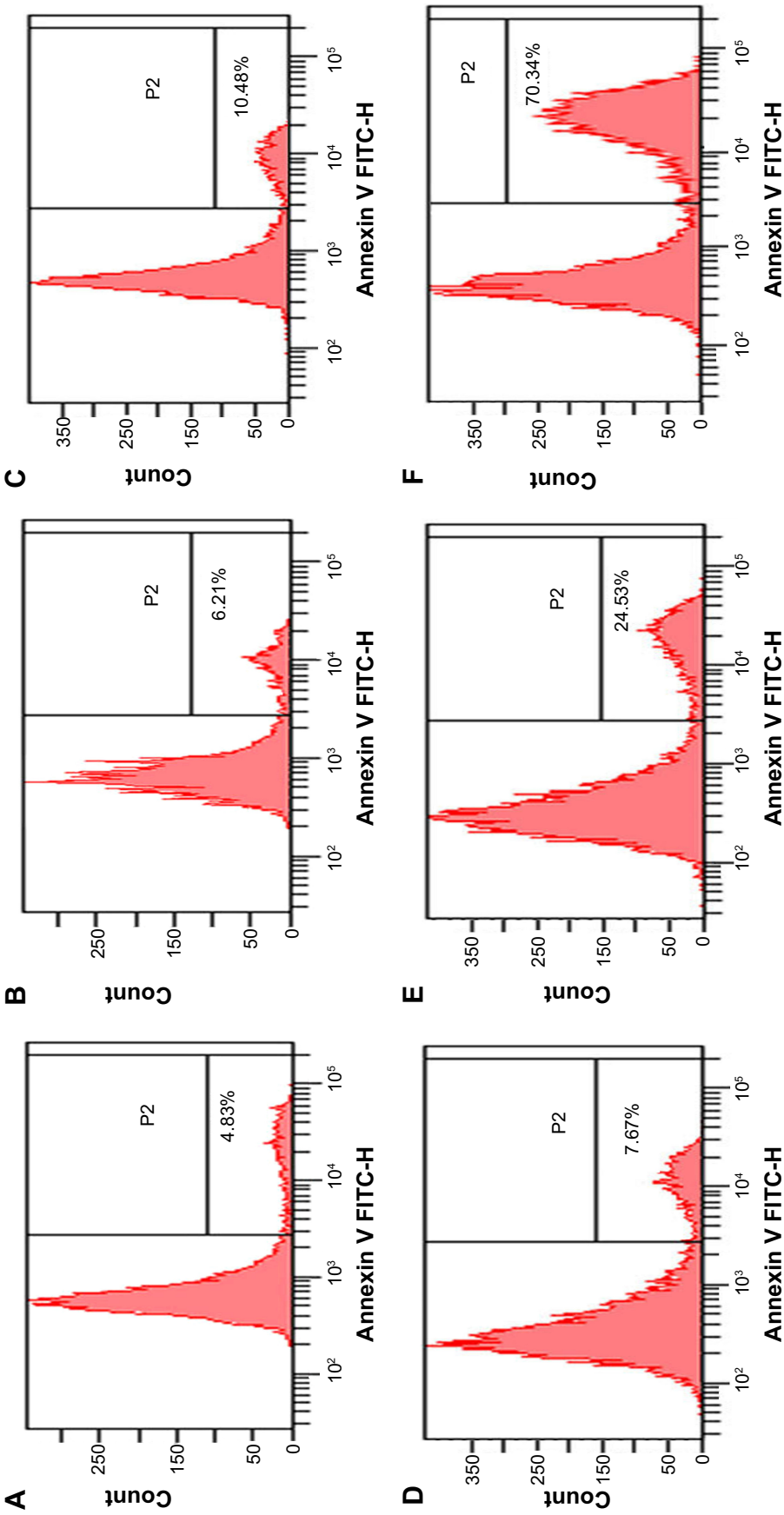

Figure 5 Apoptotic rates of RPMI-8226 cells treated for 48 hours by FCM assays. (**A**) control; (**B**) 60 mg/L DMSA-Fe_3O_4; (**C**) 2.5 nM BTZ; (**D**) 0.2 μM GA; (**E**) 2.5 nM BTZ-0.2 μM GA; (**F**) 2.5 nM BTZ-0.2 μM GA-60 mg/L DMSA-Fe_3O_4.

Abbreviations: FCM, flow cytometry; DMSA-Fe_3O_4, dimercaptosuccinic acid modified iron oxide; BTZ, bortezomib; GA, gambogic acid; BTZ-GA, bortezomib-gambogic acid; BTZ-GA/MNPs, bortezomib-gambogic acid/dimercaptosuccinic acid modified iron oxide (DMSA-Fe_3O_4) magnetic nanoparticles.

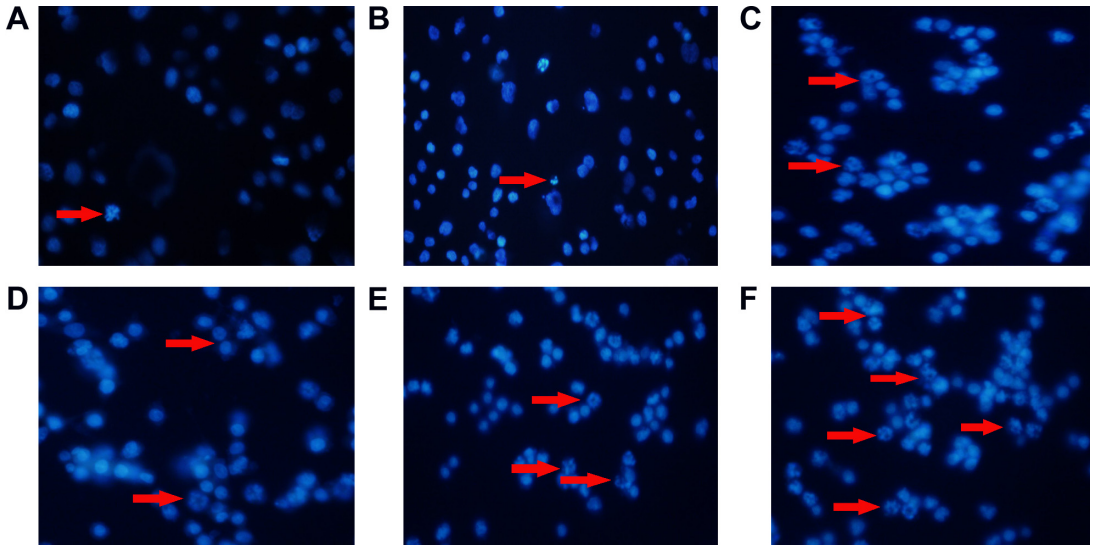

Figure 6 Morphological characterization of RPMI-8226 cells treated with and without MNPs for 48 hours by DAPI staining. The cells were visualized under fluorescence microscopy (×200). (**A**) control; (**B**) 60 mg/L DMSA-Fe_3O_4; (**C**) 2.5 nM BTZ; (**D**) 0.2 μM GA; (**E**) 2.5 nM BTZ-0.2 μM GA; (**F**) 2.5 nM BTZ-0.2 μM GA-60 mg/L DMSA-Fe_3O_4.

Note: Red arrows indicate apoptotic cells within the cell populations.

Abbreviations: DMSA-Fe_3O_4 MNPs, dimercaptosuccinic acid modified iron oxide magnetic nanoparticles; DAPI, 4,6-diamidino-2-phenylindole; BTZ, bortezomib; GA, gambogic acid; BTZ-GA, bortezomib-gambogic acid; BTZ-GA/MNPs, bortezomib-gambogic acid/dimercaptosuccinic acid modified iron oxide (DMSA-Fe_3O_4) magnetic nanoparticles.

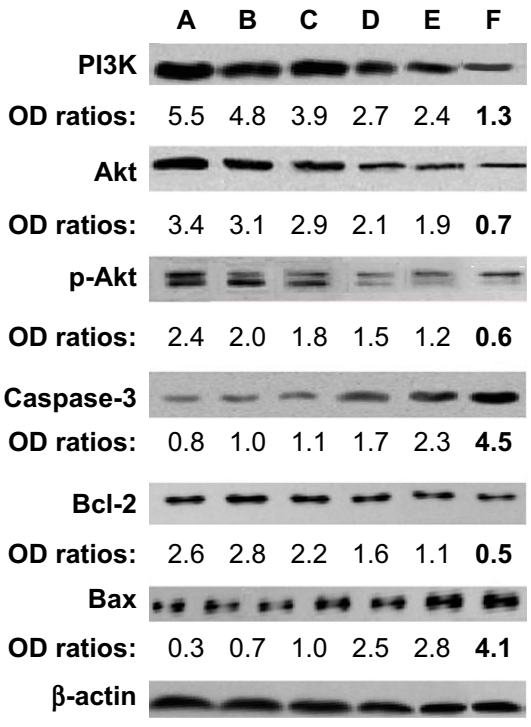

Figure 7 Expression of PI3K, Akt, p-Akt, Caspase-3, Bcl-2 and Bax protein were analyzed by Western blotting. (**A**) control (CTL); (**B**) 60 mg/L DMSA-Fe_3O_4; (**C**) 2.5 nM BTZ; (**D**) 0.2 μM GA; (**E**) 2.5 nM BTZ-0.2 μM GA; (**F**) 2.5 nM BTZ-0.2 μM GA-60 mg/L DMSA-Fe_3O_4. Bold values indicates significant difference between combination group and other groups.

Abbreviations: DMSA-Fe_3O_4 MNPs, dimercaptosuccinic acid modified iron oxide magnetic nanoparticles; BTZ, bortezomib; GA, gambogic acid; BTZ-GA, bortezomib-gambogic acid; BTZ-GA/MNPs, bortezomib-gambogic acid/dimercaptosuccinic acid modified iron oxide (DMSA-Fe_3O_4) magnetic nanoparticles.

cells and hypoxia-induced MM cells.[32] The present results showed that nontoxic concentration of BTZ at 2.5 nM with GA at 0.2 μM led to significant inhibition of cell growth in a dose-dependent manner. Furthermore, the combination of BTZ-GA/MNPs exhibited better inhibitory activity than BTZ or GA alone. These outcomes indicated that the combined application of BTZ and GA possesses a synergistic anticancer effect on RPMI-8226 cells. Considering the barriers affecting GA usage in clinical applications due to its low water solubility, we employed the hydrodynamic size of Fe_3O_4 MNPs modified with DMSA nanoparticles as drug vehicles in tumor therapy because of their active and passive accumulation in target tissues. Results of the present investigation indicated that while using DMSA-Fe_3O_4 with an average hydrodynamic size of 68.4±11.39 nm, a majority of MNPs were taken up by RPMI-8226 cells through membrane-bound vesicles and shuttled to the cytosol (Figure 2C and D). Furthermore, results indicated that there was negative charge on the surface of DMSA-MNPs or BTZ and GA solution,[26,36] hence, we deduced that BTZ and GA may have been polymerized on the surface of DMSA-MNPs nanoparticles for nanocomposites through hydrogen bond combination and not static electricity adsorption. Thus, the ability to suppress efflux pumps in the cell membrane and transport drugs into the cell might be one of the proposed mechanisms allowing MNPs to improve treatment efficiency. As a promising drug carrier for cancer

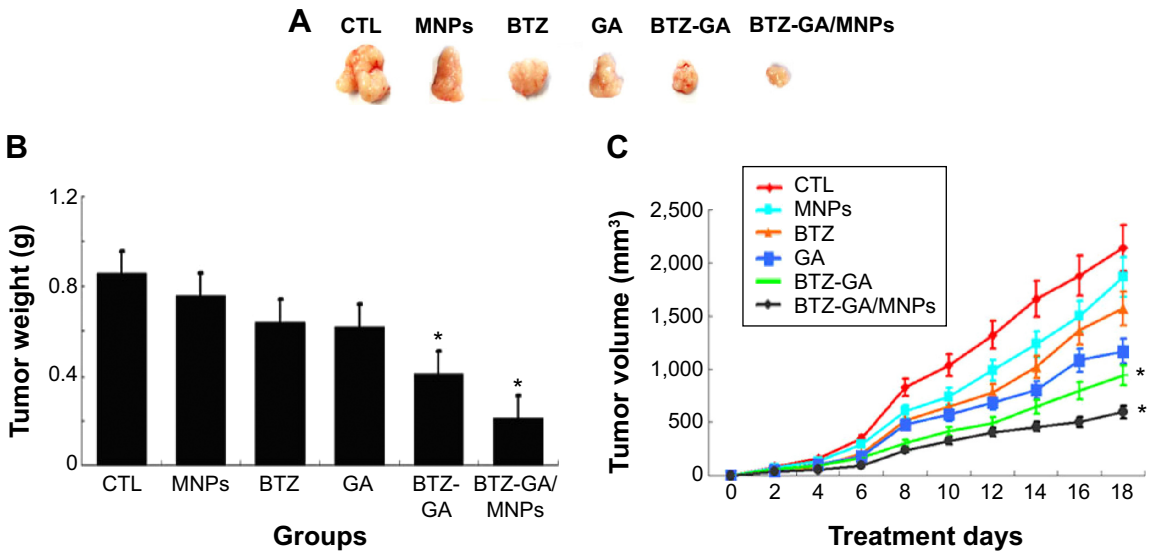

Figure 8 The change of tumor weight and volume in xenograft mouse model. (**A**) tumor size; (**B**) tumor weight and (**C**) tumor volume.
Note: *$P<0.05$ when compared with control group.
Abbreviations: CTL, control; DMSA-Fe_3O_4 MNPs, dimercaptosuccinic acid modified iron oxide magnetic nanoparticles; BTZ, bortezomib; GA, gambogic acid; BTZ-GA, bortezomib-gambogic acid; BTZ-GA/MNPs, bortezomib-gambogic acid/dimercaptosuccinic acid modified iron oxide (DMSA-Fe_3O_4) magnetic nanoparticles.

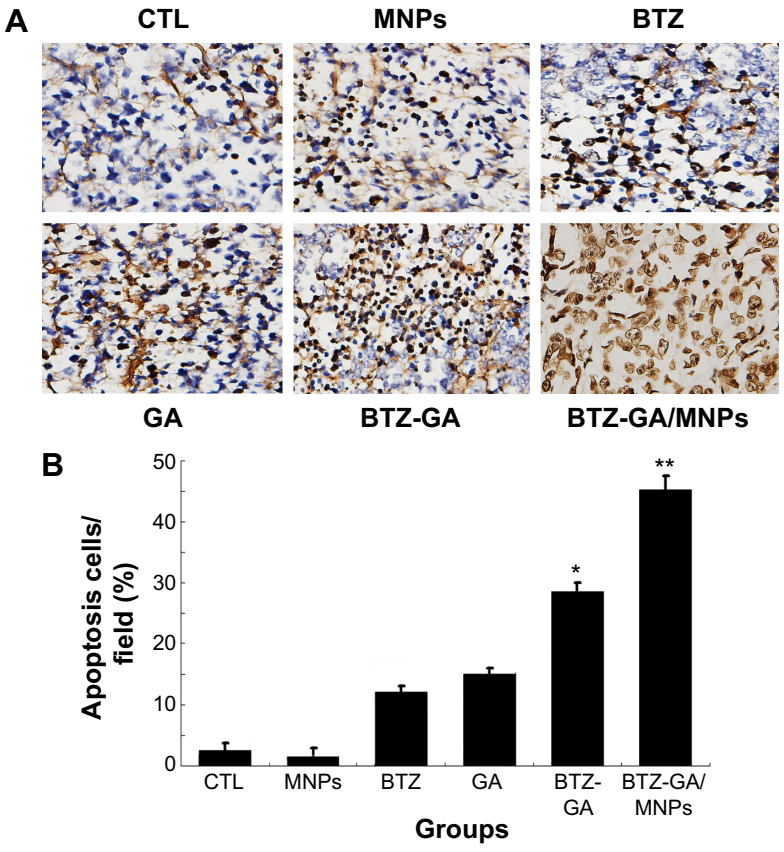

Figure 9 Apoptotic ratio of xenograft mouse tumor model was analyzed by TUNEL assay (×200). (**A**) Morphological features of RPMI-8226 cells-implanted nude mouse tumor tissue showing the induction of apoptosis (The apoptotic cells are shown in brown color). (**B**) This plot summarizes the data from panel (**A**).
Notes: *$P<0.05$ when compared with control group; **$P<0.05$ when compared with BTZ-GA group.
Abbreviations: TUNEL, terminal deoxyribonucleotidyl transferase (TdT)-mediated biotin-16-dUTP nick-end labeling; CTL, control; DMSA-Fe_3O_4 MNPs, dimercaptosuccinic acid modified iron oxide magnetic nanoparticles; BTZ, bortezomib; GA, gambogic acid; BTZ-GA, bortezomib-gambogic acid; BTZ-GA/MNPs, bortezomib-gambogic acid/dimercaptosuccinic acid modified iron oxide (DMSA-Fe_3O_4) magnetic nanoparticles.

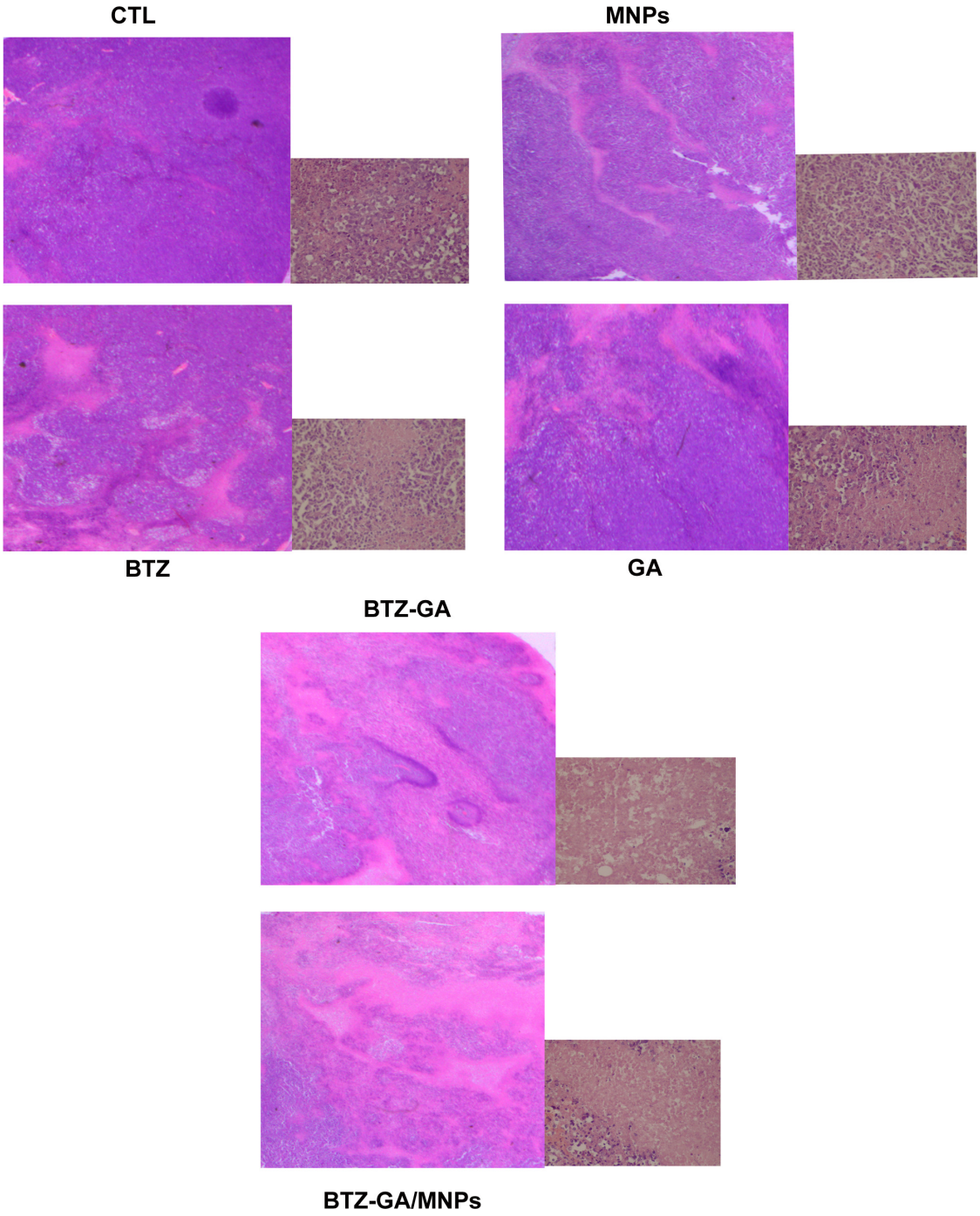

Figure 10 Tumor necrosis was checked by HE staining (×200).
Abbreviations: HE, hematoxylin and eosin; CTL, control; MNPs, 60 mg/L dimercaptosuccinic acid modified iron oxide (DMSA-Fe_3O_4) magnetic nanoparticles; BTZ, 2.5 nM bortezomib; GA, 0.2 μM gambogic acid; BTZ-GA, 2.5 nM bortezomib-0.2 μM gambogic acid; BTZ-GA/MNPs, 0.5 nM bortezomib-0.2 μM gambogic acid/60 mg/L dimercaptosuccinic acid modified iron oxide (DMSA-Fe_3O_4) magnetic nanoparticles.

therapy, the combination of DMSA-Fe_3O_4 with BTZ and GA showed better inhibitory effectiveness in MM cells.

As a result of the biological characteristics of malignant tumor, different types of antitumor agents are only able to be applied for a limited time. Merely increasing the doses does not improve the curative effect, but increases obviously the toxicity and probably increases drug resistance. Several studies indicate that the antitumor effect of a vast majority of chemotherapeutics is achieved through inducing apoptosis in tumor cells. Examples of such chemotherapeutics include anthracyclines and 5-fluorouracil.[37,38] Moreover, nontoxic concentrations of BTZ and GA increase cell accumulation in

the G_2/M phase and induce apoptosis. The apoptotic rate of RPMI-8226 cells treated with the combination of MNPs and BTZ with GA increased significantly as compared with that of BTZ and GA alone. These results were also confirmed by the typical morphological features of apoptosis in RPMI-8226 cells by DAPI staining. Notably, the shift of cell distribution into the G_2/M phase was augmented by MNPs, suggesting that MNPs synergistically enhance BTZ-GA-induced G_2/M arrest and cell apoptosis. It is also worth reminding the reader that any drugs that combat cycle-mediated drug resistance would be better chemotherapeutic agents to overcome cancer multidrug resistance. The combination of BTZ-GA/MNPs improve G_2/M phase cell cycle arrest and it could act as cell cycle-specific modulator in MM cells.

PI3K/Akt is identified as an oncogenic signal in the pathophysiology of MM and other hematological malignancies.[39] It has been previously reported that the alteration of the PI3K pathway signaling is an indicator of poor prognosis and resistance to available treatments in MM.[40] Furthermore, other researchers have proposed that the expression of $pSer^{473}$ is related with the survival ratio in primary MM cells.[41] Collectively, these data suggest that inhibiting PI3K/Akt signal pathway is an ideal target for anti-myeloma drug discovery. Results of the study showed that the combination of MNPs and BTZ with GA decreased PI3K expression and activated the $pSer^{473}$ level. Moreover, the Bcl-2/Bax ratio was decreased and Caspase-3 expression was increased. These results are partly concurrent with the fact that PI3K also regulates the expression of anti-apoptotic proteins such as Bcl-2, Mcl-1, and activated Caspase-3 and induces cell death.[42,43] The results further imply that MNPs combined with nontoxic concentrations of BTZ and GA increased the antitumor efficacy of MM cells. The combination of BTZ-GA/MNPs adjusted PI3K/Akt activation-induced cell death through various apoptotic pathways. However, the detailed mechanisms underlying the inhibition of PI3K/Akt pathway by BTZ-GA or MNPs combined with BTZ and GA are not clear so far. Further in vivo and in vitro studies are greatly warranted to support our data that uses the combination of MNPs-Fe_3O_4 with anticancer drug GA and BTZ to treat MM malignancy.

A successful anticancer treatment should have the capability to efficiently inhibit cancer cell growth in vivo. As shown in our data, MNPs or BTZ or GA alone were unable to significantly inhibit the tumor growth in RPMI-8226 tumor-bearing mice. However, the tumor size and body weight of the mice in the BTZ-GA group and the BTZ-GA/MNPs group were significantly decreased and antitumor activity greatly enhanced, suggesting the synergistic effect of the combination of BTZ-GA/MNPs in vivo. We propose that MNPs could disrupt the tumor cell membrane, so that BTZ could be delivered into the tumor cells more efficiently. Many studies also reported that the MNPs could slow down the tumor growth in nude mice, cause DNA damage, and induce cell apoptosis.[44,45] The improved antitumor activity of BTZ-GA/MNPs was further confirmed by DNA fragmentation in tumor cells after TUNEL staining. As shown in the results, a greater induction of tumor cell apoptosis was observed with BTZ-GA/MNPs compared to the other groups. In addition, BTZ-GA/MNPs resulted in the most severe tumor necrosis compared to the other formulations, while Liu et al reported that GA did not enhance or antagonized the antitumor activity of BTZ in vivo.[46] These opposing results suggest that there may be fundamental differences between cell types. Our results further suggest the outstanding antitumor efficacy of BTZ-GA/MNPs. In short, BTZ-GA/MNPs inhibit cell growth and enhance cell cycle G_2/M arrest and cell apoptosis through PI3K/Akt pathway in vitro and in vivo MM xenograft models. Based on the outcome of this study, it is suggested that combination therapy triggers synergistic anti-MM activity, and it could be used as an effective cancer therapeutic strategy to overcome BTZ resistance.

Conclusion

In conclusion, our overall findings strongly demonstrate that MNPs combination with nontoxic concentration of BTZ and GA exhibited better synergistic effect by inducing G_2/M phase cell cycle arrest and apoptosis via upregulation of proapoptotic protein expression Bax, Caspase-3 and downregulation of antiapoptotic proteins PI3K, Bcl-2, total-Akt, $pSer^{473}$ in vivo and in vitro. These findings highlight the potential use of BTZ-GA/MNPs as a chemotherapeutic modulator for target treating human MM.

Acknowledgments

This work was supported financially by National High Technology Research and development Program 863 of People's Republic of China (No 2012AA022703), National Natural Science Funds of People's Republic of China (No 81170492), Key Medical Program of Jiangsu Province Department of Technology (No BL2014078), and the Tianjin City Health Industry Key Project (No 12KG109).

Disclosure

The authors report no conflicts of interest in this work.

References

1. Chang WJ, Glebov O, Bergsagel PL, Kuehl WM. Genetic events in the pathogenesis of multiple myeloma. *Best Pract Res Clin Haematol*. 2007;20:571–596.
2. Kyle RA, Rajkumar SV. Multiple myeloma. *Blood*. 2008;111: 2962–2972.
3. Palumbo A, Anderson K. Multiple myeloma. *N Engl J Med*. 2011; 364:1046–1060.
4. Laubach JP, Mitsiades CS, Mahindra A, et al. Novel therapies in the treatment of multiple myeloma. *J Natl Compr Canc Netw*. 2009;7: 947–960.
5. Ma MH, Yang HH, Parker K, et al. The proteasome inhibitor PS-341 markedly enhances sensitivity of multiple myeloma tumor cells to chemotherapeutic agents. *Clin Cancer Res*. 2003;9:1136–1144.
6. Hideshima T, Richardson P, Chauhan D, et al. The proteasome inhibitor PS-341 inhibits growth, induces apoptosis, and overcomes drug resistance in human multiple myeloma cells. *Cancer Res*. 2001;61: 3071–3076.
7. Siegel R, Naishadham D, Jemal A. Cancer statistics. *CA Cancer J Clin*. 2012;62:10–29.
8. Van Besien K. Current status of allogeneic transplantation for aggressive non-Hodgkin lymphoma. *Curr Opin Oncol*. 2011;23:681–691.
9. Fox E, Razzouk BI, Widemann BC, et al. Phase 1 trial and pharmacokinetic study of arsenic trioxide in children and adolescents with refractory or relapsed acute leukemia, including acute promyelocytic leukemia or lymphoma. *Blood*. 2008;111:566–573.
10. Hideshima T, Neri P, Tassone P, et al. MLN120B, a novel IkappaB kinase beta inhibitor, blocks multiple myeloma cell growth in vitro and in vivo. *Clin Cancer Res*. 2006;12:5887–5994.
11. Takamatsu Y, Sunami K, Hata H, et al; The Kyushu Hematology Organization for Treatment Study Group. A phase I study of bortezomib in combination with doxorubicin and intermediate-dose dexamethasone (iPAD therapy) for relapsed or refractory multiple myeloma. *Int J Hematol*. 2010;92:503–509.
12. Takamatsu Y, Sunami K, Muta T, et al; The Kyushu Hematology Organization for Treatment Study Group. Bortezomib, doxorubicin and intermediate-dose dexamethasone (iPAD) therapy for relapsed or refractory multiple myeloma: a multicenter phase 2 study. *Int J Hematol*. 2013;98:179–185.
13. Yang LJ, Chen Y. New targets for the antitumor activity of gambogic acid in hematologic malignancies. *Acta Pharmacol Sin*. 2013; 34:191–198.
14. Li X, Liu S, Huang H, et al. Gambogic acid is a tissue-specific proteasome inhibitor in vitro and in vivo. *Cell Rep*. 2013;3:211–222.
15. Wang Y, Xiang W, Wang M, et al. Methyl jasmonate sensitizes human bladder cancer cells to gambogic acid-induced apoptosis through down-regulation of EZH2 expression by miR-101. *Br J Pharmacol*. 2014;171: 618–635.
16. Duan D, Zhang B, Yao J, et al. Gambogic acid induces apoptosis in hepatocellular carcinoma SMMC-7721 cells by targeting cytosolic thioredoxin reductase. *Free Radic Biol Med*. 2014;69:15–25.
17. Koppolu B, Bhavsar Z, Wadajkar AS, et al. Temperature-sensitive polymercoated magnetic nanoparticles as a potential drug delivery system for targeted therapy of thyroid cancer. *J Biomed Nanotechnol*. 2012;8: 983–990.
18. Chanana M, Mao ZW, Wang DY. Using polymers to make up magnetic nanoparticles for biomedicine. *J Biomed Naonotechnol*. 2009;5: 652–668.
19. Mbeh DA, França R, Merhi Y, et al. In vitro biocompatibility assessment of functionalized magnetite nanoparticles: biological and cytotoxicological effects. *J Biomed Mater Res*. 2012;100:1637–1646.
20. Qiao RR, Zeng JF, Jia QJ, et al. Magnetic iron oxide nanoparticle an important cornerstone of MR molecular imaging of tumors. *Acta Phys Chim Sin*. 2012;28:993–1001.
21. Zhang X, Jiang L, Zhang C, et al. A silicon dioxide modified magnetic nanoparticles labeled flow strip for HBs antigen. *J Biomed Nanotechnol*. 2011;7:776–781.
22. Ma C, Li C, He N, et al. Preparation and characterization of monodisperse core–shell Fe_3O_4@SiO_2 Microspheres and its application for magnetic separation of nucleic acids from *E. coli* BL21. *J Biomed Nanotechnol*. 2012;8:1000–1005.
23. Oliveira RR, Ferreira FS, Cintra ER, Branquinho LC, Bakuzis AF, Lima EM. Magnetic nanoparticles and rapamycin encapsulated into polymeric nanocarriers. *J Biomed Nanotechnol*. 2012;8:193–201.
24. Singh R, Nalwa HS. Medical applications of nanoparticles in biological imaging, cell labeling, antimicrobial agents and anticancer nanodrugs. *J Biomed Nanotechnol*. 2011;7:489–503.
25. Cai X, Cai X, Wang C, et al. Antitumor efficacy of DMSA modified Fe_3O_4 magnetic nanoparticles combined with arsenic trioxide and adriamycin in Raji Cells. *J Biomed Nanotechnol*. 2014;10:251–261.
26. Chen ZP, Zhang Y, Xu K, Xu RZ, Liu JW, Gu N. Stability of hydrophilic magnetic nanoparticles under biologically relevant conditions. *J Nanosci Nanotechnol*. 2008;8:6260–6265.
27. Chen ZP, Zhang Y, Xia JG, et al. Preparation and characterization of water-soluble monodisperse magnetic iron nanoparticles via surface double-exchange with DMSA. *Colloid Surface*. 2008;316:210–216.
28. Jiang Z, Chen BA, Xia GH, et al. The reversal effect of magnetic Fe_3O_4 nanoparticles loaded with cisplatin on SKOV3/DDP ovarian carcinoma cells. *Int J Nanomed*. 2009;4:107–114.
29. Zhao L, Guo QL, You QD, Wu ZQ, Gu HY. Gambogic acid induces apoptosis and regulates expressions of Bax and Bcl-2 protein in human gastric carcinoma MGC-803 cells. *Biol Pharm Bull*. 2004;27: 998–1003.
30. Cheng J, Wu WW, Chen BA, et al. Effect of magnetic nanoparticles of Fe_3O_4 and 5-bromotetrandrine on reversal of multidrug resistance in K562/A02 leukemic cells. *Int J Nanomed*. 2009;4:209–216.
31. Lowry OH, Rosebrough NJ, Farr AL, Randall RJ. Protein measurement with the Folin phenol reagents. *J Biol Chem*. 1951;193:265–275.
32. Wang F, Zhang W, Guo L, et al. Gambogic acid suppresses hypoxia-induced hypoxia-inducible factor-1/vascular endothelial growth factor expression via inhibiting phosphatidylinositol 3-kinase/Akt/mammalian target protein of rapamycin pathway in multiple myeloma cells. *Cancer Sci*. 2014;105(8):1063–1070.
33. Chen B, Liang Y, Wu W, et al. Synergistic effect of magnetic nanoparticles of Fe_3O_4 with gambogic acid on apoptosis of K562 leukemia cells. *J Biomed Nanotechnol*. 2009;4:251–259.
34. Wang X, Deng R, Lu Y, et al. Gambogic acid as a non-competitive inhibitor of ATP-binding cassette transporter B1 reverses the multidrug resistance of human epithelial cancers by promoting ATP-binding cassette transporter B1 protein degradation. *Basic Clin Pharmacol Toxicol*. 2013;112:25–33.
35. Qi Q, You Q, Gu H, et al. Studies on the toxicity of gambogic acid in rats. *J Ethnopharmacol*. 2008;117:433–438.
36. Valois CR, Braz JM, Nunes ES, et al. The effect of DMSA-functionalized magnetic nanoparticles on transendothelial migration of monocytes in the murine lung via aβ2 integrin-dependent pathway. *Biomaterials*. 2010;31:366–374.
37. Barry MA, Behnke CA, Eastman A. Activation of programmed cell death (apoptosis) by cisplatin, other anticancer drugs, toxins and hyperthermia. *Biochem Pharmacol*. 1990;40:2353–2362.
38. Lu H, Yuan GX, He QH. Rapid analysis of anthracycline antibiotics doxorubicin and daunorubicin by microchip capillary electrophoresis. *Microchem J*. 2009;92:170–175.
39. Harvey RD, Lonial S. PI3 kinase/AKT pathway as a therapeutic target in multiple myeloma. *Future Oncol*. 2007;3:639–647.
40. Ikeda H, Hideshima T, Fulciniti M, et al. PI3K/p110{delta} is a novel therapeutic target in multiple myeloma. *Blood*. 2010;116: 1460–1468.
41. Hsu J, Shi Y, Krajewski S, et al. The AKT kinase is activated in multiple myeloma tumor cells. *Blood*. 2001;98:2853–2855.
42. Mao X, Cao B, Wood TE, et al. A small-molecule inhibitor of D-cyclin transactivation displays preclinical efficacy in myeloma and leukemia via phosphoinositide 3-kinase pathway. *Blood*. 2011;117:1986–1997.

43. Hennessy BT, Smith DL, Ram PT, Lu Y, Mills GB. Exploiting the PI3K/AKT pathway for cancer drug discovery. *Nat Rev Drug Discov*. 2005;4:988–1004.
44. Tofani S, Barone D, Berardelli M, et al. Static and ELF magnetic fields enhance the in vivo antitumor efficacy of cisplatin against Lewis lung carcinoma, but not of cyclophosphamide against B16 melanotic melanoma. *Pharmacol Res*. 2003;48:83–90.
45. Jajte J, Grzegorczyk J, Zmyslony M, Rajkowska E. Effect of 7mT static magnetic field and iron ions on rat lymphocytes: apoptosis, necrosis and free radical processes. *Bioelectrochemistry*. 2002;57:107–111.
46. Liu N, Huang H, Xu L, et al. The combination of proteasome inhibitors bortezomib and gambogic acid triggers synergistic cytotoxicity in vitro but not in vivo. *Toxicology Let*. 2014;224:333–340.